OPEN ACCESS

Original research

Roseburia intestinalis generated butyrate boosts anti-PD-1 efficacy in colorectal cancer by activating cytotoxic CD8$^+$ T cells

Xing Kang,[1] Changan Liu,[1] Yanqiang Ding,[1] Yunbi Ni,[2] Fenfen Ji,[1] Harry Cheuk Hay Lau ,[1] Lanping Jiang,[1] Joseph JY Sung ,[1,3] Sunny H Wong ,[1,3] Jun Yu [1]

► Additional supplemental material is published online only. To view, please visit the journal online (http://dx.doi.org/10.1136/gutjnl-2023-330291).

[1]Institute of Digestive Disease and Department of Medicine and Therapeutics, State Key Laboratory of Digestive Disease, Li Ka Shing Institute of Health Sciences, The Chinese University of Hong Kong, Shatin, Hong Kong
[2]Department of Anatomical and Cellular Pathology, Faculty of Medicine, The Chinese University of Hong Kong, Shatin, Hong Kong
[3]Lee Kong Chian School of Medicine, Nanyang Technological University, Singapore

Correspondence to
Dr Jun Yu, Department of Medicine and Therapeutics, The Chinese University of Hong Kong, Shatin, Hong Kong; junyu@cuhk.edu.hk and Dr Sunny H Wong, Lee Kong Chian School of Medicine, Nanyang Technology University, Singapore, Singapore; sunny.wong@ntu.edu.sg

Received 15 May 2023
Accepted 21 June 2023
Published Online First 25 July 2023

To cite: Kang X, Liu C, Ding Y, *et al*. *Gut* 2023;**72**:2112–2122.

ABSTRACT

Objective *Roseburia intestinalis* is a probiotic species that can suppress intestinal inflammation by producing metabolites. We aimed to study the role of *R. intestinalis* in colorectal tumourigenesis and immunotherapy.

Design *R. intestinalis* abundance was evaluated in stools of patients with colorectal cancer (CRC) (n=444) and healthy controls (n=575). The effects of *R. intestinalis* were studied in *Apc*$^{Min/+}$ or azoxymethane (AOM)-induced CRC mouse models, and in syngeneic mouse xenograft models of CT26 (microsatellite instability (MSI)-low) or MC38 (MSI-high). The change of immune landscape was evaluated by multicolour flow cytometry and immunohistochemistry staining. Metabolites were profiled by metabolomic profiling.

Results *R. intestinalis* was significantly depleted in stools of patients with CRC compared with healthy controls. *R. intestinalis* administration significantly inhibited tumour formation in *Apc*$^{Min/+}$ mice, which was confirmed in mice with AOM-induced CRC. *R. intestinalis* restored gut barrier function as indicated by improved intestinal permeability and enhanced expression of tight junction proteins. Butyrate was identified as the functional metabolite generated by *R. intestinalis*. *R. intestinalis* or butyrate suppressed tumour growth by inducing cytotoxic granzyme B$^+$, interferon (IFN)-γ^+ and tumour necrosis factor (TNF)-α^+ CD8$^+$ T cells in orthotopic mouse models of MC38 or CT26. *R. intestinalis* or butyrate also significantly improved antiprogrammed cell death protein 1 (anti-PD-1) efficacy in mice bearing MSI-low CT26 tumours. Mechanistically, butyrate directly bound to toll-like receptor 5 (TLR5) receptor on CD8$^+$ T cells to induce its activity through activating nuclear factor kappa B (NF-κB) signalling.

Conclusion *R. intestinalis* protects against colorectal tumourigenesis by producing butyrate, which could also improve anti-PD-1 efficacy by inducing functional CD8$^+$ T cells. *R. intestinalis* is a potential adjuvant to augment anti-PD-1 efficacy against CRC.

WHAT IS ALREADY KNOWN ON THIS TOPIC

⇒ Gut microbiome and metabolites are associated with colorectal cancer (CRC) tumourigenesis and immunotherapeutic response.
⇒ *Roseburia intestinalis* is a probiotic species that can suppress intestinal inflammation by producing metabolites.

WHAT THIS STUDY ADDS

⇒ *R. intestinalis* is depleted in patients with CRC compared with healthy controls by faecal metagenomic sequencing.
⇒ *R. intestinalis* administration significantly inhibits tumour formation and restores gut barrier function in multiple CRC mouse models.
⇒ Butyrate is the functional metabolite produced by *R. intestinalis* identified by non-target, target metabolomic profiling and biofunctional investigations.
⇒ Butyrate inhibites CRC tumourigenesis, and in particular boosts antiprogrammed cell death protein 1 (anti-PD-1) efficacy by enhancing the activity of cytotoxic CD8$^+$ T cells in mice.
⇒ Mechanistically, butyrate directly binds to toll-like receptor 5 (TLR5) receptor on CD8$^+$ T cells to induce its activity through activating nuclear factor kappa B (NF-κB) signalling.

HOW THIS STUDY MIGHT AFFECT RESEARCH, PRACTICE OR POLICY

⇒ *R. intestinalis* protects against colorectal tumourigenesis by producing butyrate.
⇒ *R. intestinalis* and its generated butyrate improve anti-PD-1 efficacy by inducing functional CD8$^+$ T cells.
⇒ *R. intestinalis* is a potential adjuvant therapy to augment anti-PD-1 efficacy against CRC.

INTRODUCTION

Colorectal cancer (CRC) is the third major cancer type and a major cause of cancer-related death worldwide.[1] Despite the high response rate to immune checkpoint blockade in patients with different cancers, the efficacy of immunotherapy against CRC is limited.[2] Clinical evidence demonstrated that only patients with CRC with microsatellite instability (MSI)-high subtype could respond to programmed cell death protein 1 (PD-1) inhibitor,[3] which only accounts for 10%–15% of total CRC cases.[4] In contrast, most CRC tumours are microsatellite stable (MSS), thus presenting a major challenge for immunotherapy against the

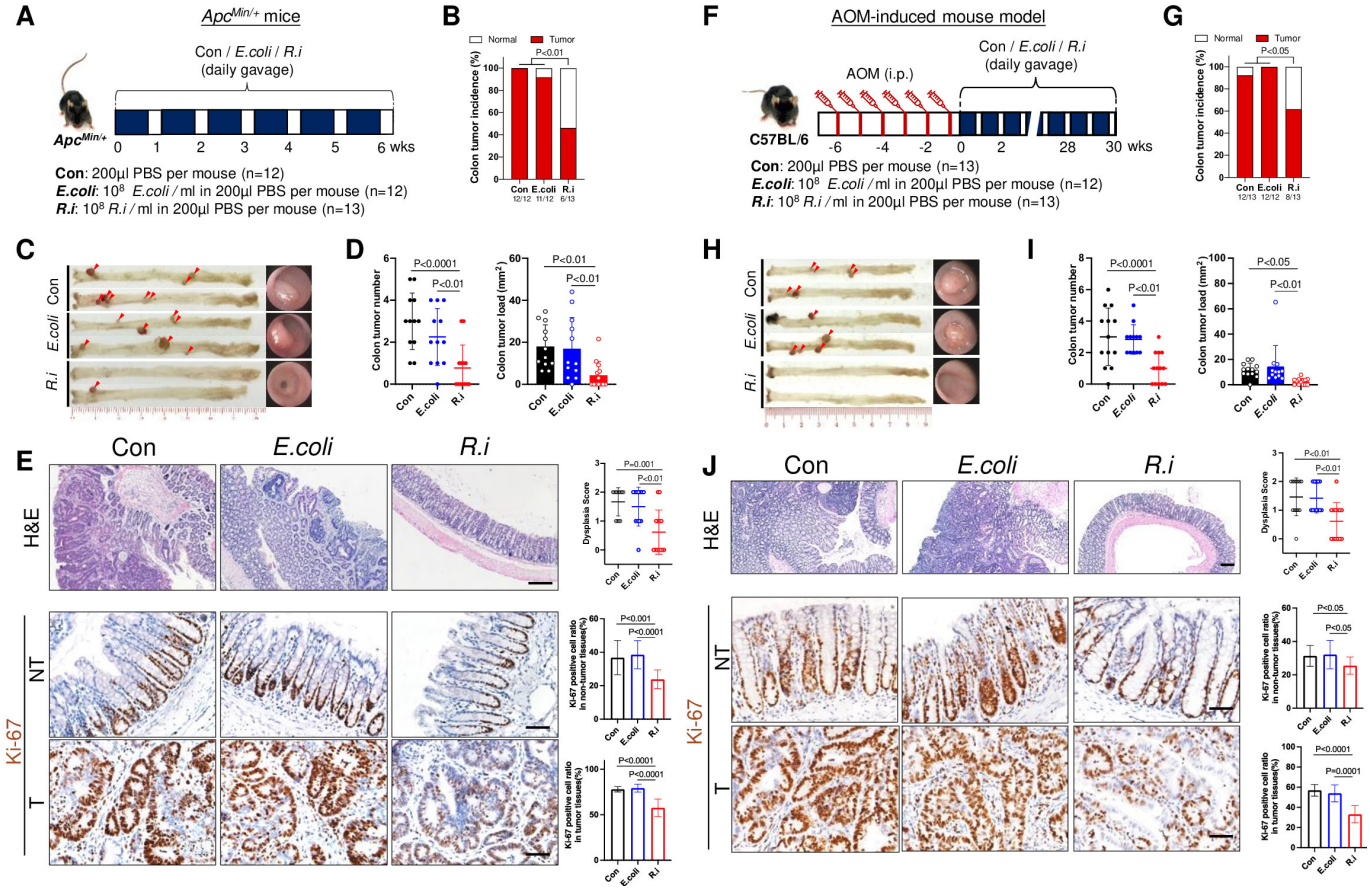

Figure 1 *Roseburia intestinalis* (*R.i*) reduces colorectal carcinogenesis in *Apc*$^{Min/+}$ and azoxymethane (AOM)-induced mice. (A) Schematic diagram showing the experimental design and timeline of *Apc*$^{Min/+}$ mice experiment. (B) Representative colonic morphologies (left panel) and colonoscopy video captures (right panel) of *Apc*$^{Min/+}$ mice. Colon tumour incidence (C), colon tumour number and colon tumour load (total tumour area, mm^2) (D) of *Apc*$^{Min/+}$ mice. (E) Representative H&E staining images (scale bar=200 µm) and Ki-67 immunohistochemistry (IHC) staining (scale bar=50 µm) of *Apc*$^{Min/+}$ mice. (F) Schematic diagram showing the experimental design and timeline of AOM-induced mice. (G) Representative colonic morphologies (left panel) and colonoscopy video captures and incidence (right panel) of AOM-induced mice. Colon tumour incidence (H), colon tumour number and colon tumour load (total tumour area, mm^2) (I) of AOM-induced mice. (J) Representative H&E staining images (scale bar=200 µm) and Ki-67 IHC staining (scale bar=50 µm) of AOM-induced mice. Con, control; *E. coli*; *Escherichia coli*; PBS, phosphate-buffered saline.

majority of patients with CRC. Given that CD8$^+$ T cells play an essential role in antitumour immunity, promoting functional CD8$^+$ T cell infiltration to the tumour microenvironment may improve immunotherapy efficacy in patients with CRC, especially for those with MSS subtype. The gut microbiota is known to be associated with the efficacy of cancer immunotherapy by modulating host antitumour immune response.[5] For instance, a depleted microbiota by antibiotics or in germ-free mice was irresponsive to immunotherapy, whereas oral supplementation of bacteria or faecal microbiota transplantation to these resistance mice restored immunotherapy response.[6 7] Nevertheless, whether and how certain bacteria improve immunotherapy efficacy in patients with CRC remain largely unclear.

Metabolites produced by the gut microbiota have been shown to influence the development of CRC.[8] Butyrate, as one of the essential bacterial metabolites,[9] its concentration is negatively correlated with CRC incidence.[10] Meanwhile, several butyrate-producing bacteria such as *Roseburia* were depleted in patients with CRC.[10] In particular, *Roseburia intestinalis*, a Gram-positive, obligate anaerobic, butyrate-producing bacterium, was first isolated from human faeces in 2002,[11] and its metabolites have been shown to prevent intestinal inflammation.[12] These data prompted us to investigate whether *R. intestinalis* and its metabolites could contribute to the suppression of colorectal tumourigenesis as well as improving immunotherapy efficacy against CRC. In this study, the protective role of *R. intestinalis* in CRC was investigated in multiple mouse models. We found that *R. intestinalis* produced butyrate which could directly boost cytotoxic CD8$^+$ T cell function through toll-like receptor 5 (TLR5)-dependent nuclear factor kappa B (NF-κB) signalling. *R. intestinalis* also restricted both MSI-high and MSS orthotopic tumour growth by modulating antitumour CD8$^+$ T cell response. Collectively, our findings suggested that *R. intestinalis* and its metabolite butyrate have potential clinical impact in improving immunotherapy efficacy in patients with CRC.

MATERIALS AND METHODS

Mouse models

Two CRC mouse models, transgenic *Apc*$^{Min/+}$ and carcinogen azoxymethane (AOM)-induced, were established in this study. The intestinal adenoma spontaneous mouse strain C57BL/6J-*Apc*^{Min}/J (The Jackson Laboratory, Maine, USA) was orally treated with 1×10^8 colony-forming unit of *R. intestinalis* daily at the age of 6 weeks, for consecutive 6 weeks. The same amount of *Escherichia coli* MG1665 or phosphate-buffered saline (PBS)

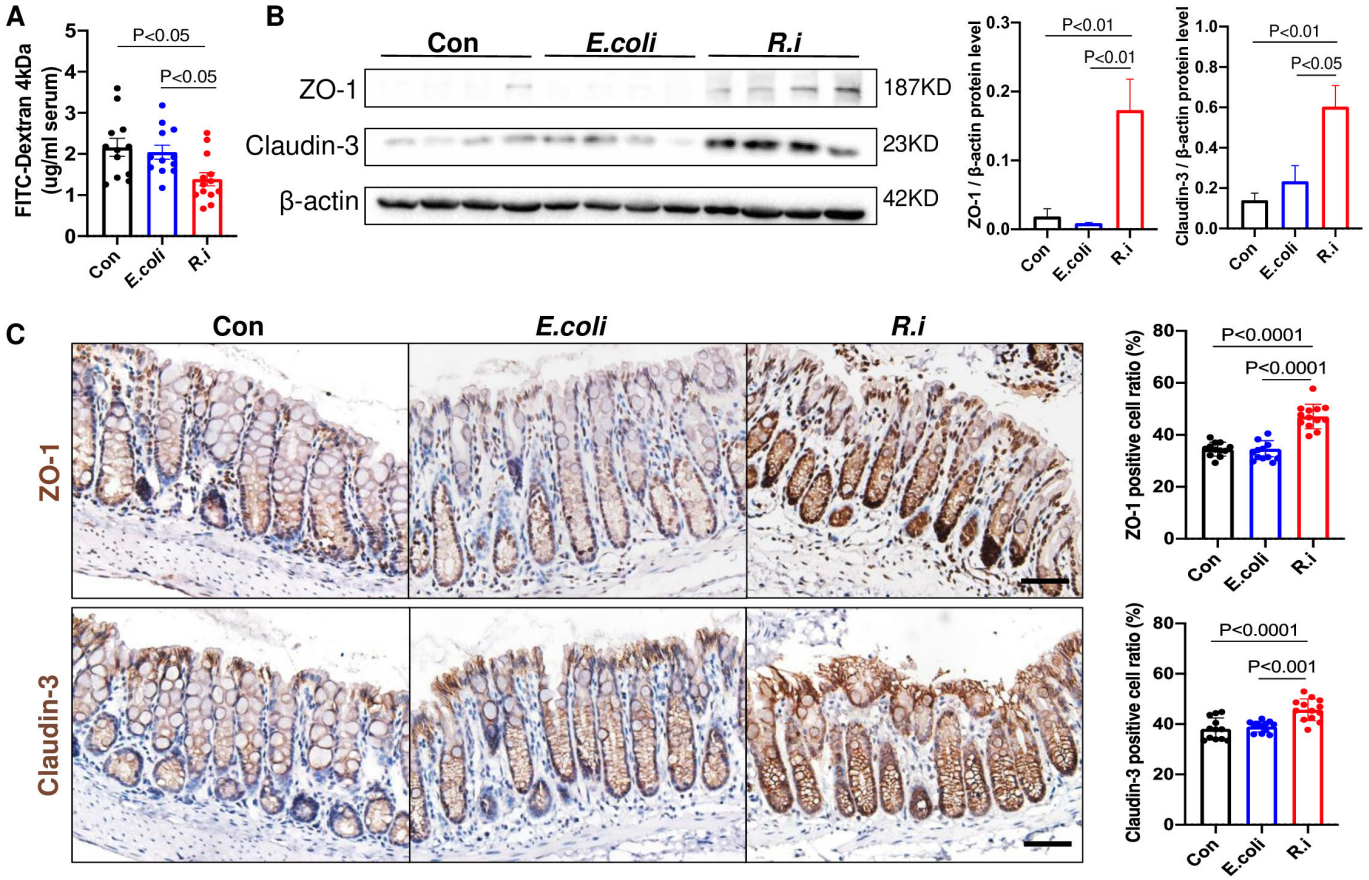

Figure 2 *Roseburia intestinalis (R.i)* enhances epithelial barrier functions in $Apc^{Min/+}$ mice. (A) FITC-dextran (4 kDa) concentration (ng/mL) in $Apc^{Min/+}$ mice serum. (B) Expression levels of tight junction proteins ZO-1 and claudin-3 determined by western blot analysis in colon tissues of $Apc^{Min/+}$ mice. (C) Representative ZO-1 and claudin-3 immunohistochemistry staining images (scale bar=50 µm). Con, control; *E. coli, Escherichia coli;* FITC, fluorescein isothiocyanate; ZO-1, zonula occludens-1.

was used as bacterial control or negative control, respectively. For another tumourigenesis model, six doses of AOM (A5486, Sigma-Aldrich, Delaware, USA) were injected into C57BL/6 mice aged 6 weeks to induce sporadic tumour development. AOM-injected mice received the same treatment as in $Apc^{Min/+}$ mouse model, which initiated 1 week after the last AOM injection and lasted for 30 weeks.

For orthotopic mouse models, MSI-high type CRC cell line MC38 (5×10^5 cells in 10 µL Matrigel (354248, Corning, Virginia) per mouse) or mouse MSS type CRC cell line CT26 was orthotopically implanted into the rectum of male C57BL/6 or BALB/c mice aged 5–6 weeks, respectively. When the tumour was established or 3 days after implantation, mice were started with *R. intestinalis, E. coli* or sodium butyrate (150 mM in drinking water, 303410, Sigma-Aldrich) daily treatment. One week after implantation, antimouse PD-1 monoclonal antibody (BP0146, clone: RMP1-14, Bio X Cell, New Hampshire, USA) or control IgG (BP0089, clone: 2A-3, Bio X Cell) was administered into mice by intraperitoneal injection every 3 days (100 µg per mouse, total of five injections).

T cell isolation and activation

T cells isolated from healthy human peripheral blood mononuclear cells (PBMC) using immunomagnetic negative selection kit (17951, STEMCELL Technologies, Canada) according to manufacturer's instructions. Isolated T cells were then cultured in RPMI-1640 medium supplied with human CD3/CD28 magnet beads (11 161D, Thermo Fisher Scientific) and 30 U/mL recombinant human IL-2 (589104, BioLegend) for expansion and activation for 3 days. Mouse T cells were isolated from the spleen of naïve mice and purified with Mouse T cell isolation kit (19851, Thermo Fisher Scientific), which were then cultured in RPMI-1640 medium with mouse CD3/CD28 beads (11 456D, Thermo Fisher Scientific) and 30 U/mL recombinant mouse IL-2 (575404, BioLegend).

Immune cell characterisation by flow cytometry

Mouse tumour tissues were minced and digested in PBS containing 0.5 mg/mL collagenase IV and 0.25 mg/mL DNase I at 37°C for 30 min. The cell suspension was then filtered through 70 µm cell strainers and resuspended in 1% bovine serum albumin for surface marker staining. For isolated human T cells after treatment (*R. intestinalis cultured medium* (*R.i* CM), sodium butyrate or TLR5 inhibitor TH1020 (HY-116961, MedChemExpress, New Jersey, USA)), they were stimulated with 30 ng/mL phorbol myristate acetate (PMA), 1 µg/mL ionomycin and 2.5 µg/mL monensin in RPMI-1640 medium at 37°C for 4 hours. After surface staining, cells were fixed by transcription factor fixation/permeabilisation buffer (00-5521-00, Invitrogen, UK), followed by intracellular cytokine staining in 1×permeabilisation buffer (00-8333-56, Invitrogen). Granzyme B, interferon (IFN)-γ, tumour necrosis factor (TNF)-α negative cells were gated in $CD8^+$ T cells ($CD45^+$ $CD3^+$ $CD8^+$) without intracellular staining. Flow cytometry was performed on FACSAria cell sorter (BD Biosciences). Data were analysed by FlowJo V.10.4. Antibodies used in this study are listed in online supplemental

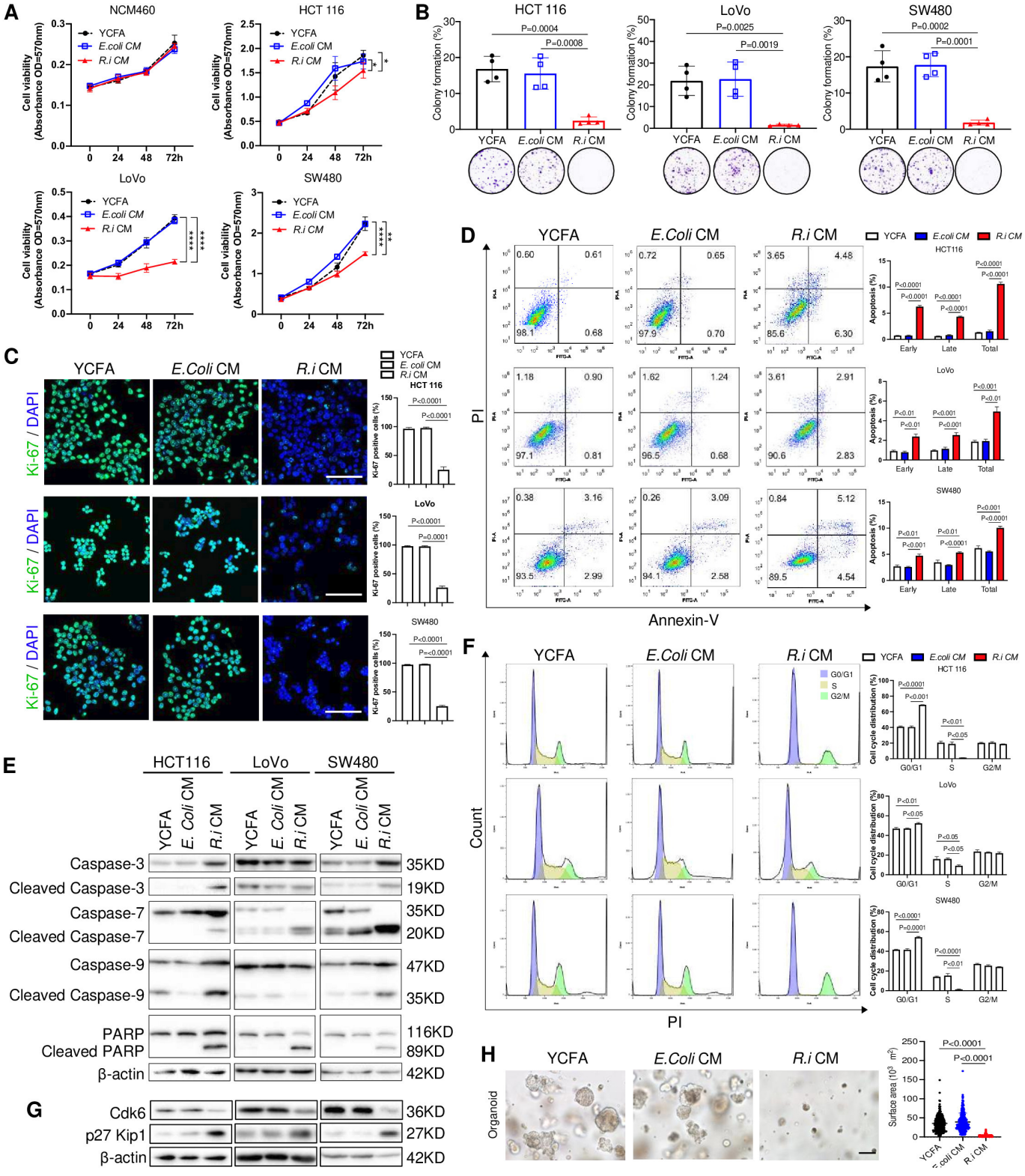

Figure 3 *Roseburia intestinalis cultured medium* (*R.i* CM) exhibits tumour-suppressive effects in vitro. (A) *R.i* CM (5%) reduced the colonic cell viability, except NCM460. *Escherichia coli* conditioned medium (*E. coli* CM) and yeast casitone fatty acids broth (YCFA) were used as control. (B) *R.i* CM (5%) suppressed the colony formation of colorectal cancer (CRC) cells. (C) *R.i* CM reduced CRC cell Ki-67 expression levels determined by immunocytochemistry. (D) *R.i* CM increased CRC cell apoptosis. (E) *R.i* CM induced CRC cell apoptosis of CRC cells by cleaved caspase-3, cleaved caspase-7, cleaved caspase-9 and cleaved poly (ADP-ribose) polymerase (PARP) expression. (F) *R.i* CM inhibited CRC cell cycle G1/S transition. (G) *R.i* CM induced G1 arrest by Cdk6 downregulation and p27 Kip1 upregulation. (H) *R.i* CM inhibited the growth of the organoid derived from a patient with CRC.

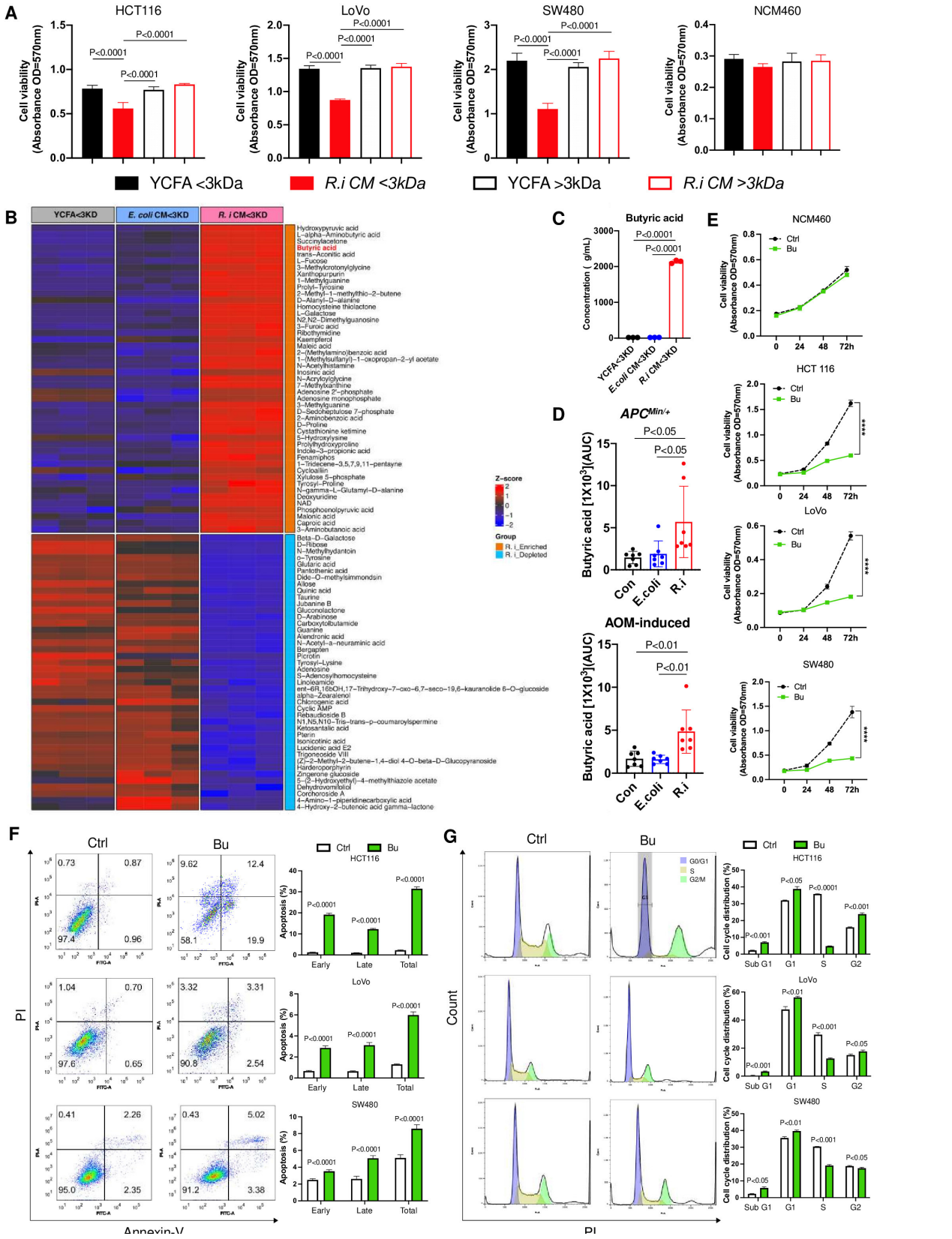

Figure 4 The tumour-suppressive component produced by *Roseburia intestinalis* is butyric acid. (A) The efficient components in *R. intestinalis cultured medium* (*R.i* CM) are <3 kDa. (B) The *R.i* CM <3 kDa fraction was assessed by untargeted liquid chromatography-tandem mass spectrometry (LC-MS/MS) analysis and butyric acid was identified as the candidate tumour-suppressive molecule. (C) Butyrate acid concentration (μg/mL) in *R.i* CM <3 kDa was determined by targeted short chain fatty acid gas chromatography-mass spectrometry (GC-MS) analysis. (D) Relative concentration of butyrate acid (area under curve (AUC)) in $Apc^{Min/+}$ *and* azoxymethane (AOM)-induced mice faeces was determined by GC-MS analysis. (E) Comparable dosage (1 mM) of butyrate in *R.i* CM reduced the colonic cell viability, except NCM460. (F) Butyrate-induced colorectal cancer (CRC) cell apoptosis. (G) Butyrate inhibited CRC cell cycle G1/S transition. Con, control; *E. coli, Escherichia coli*.

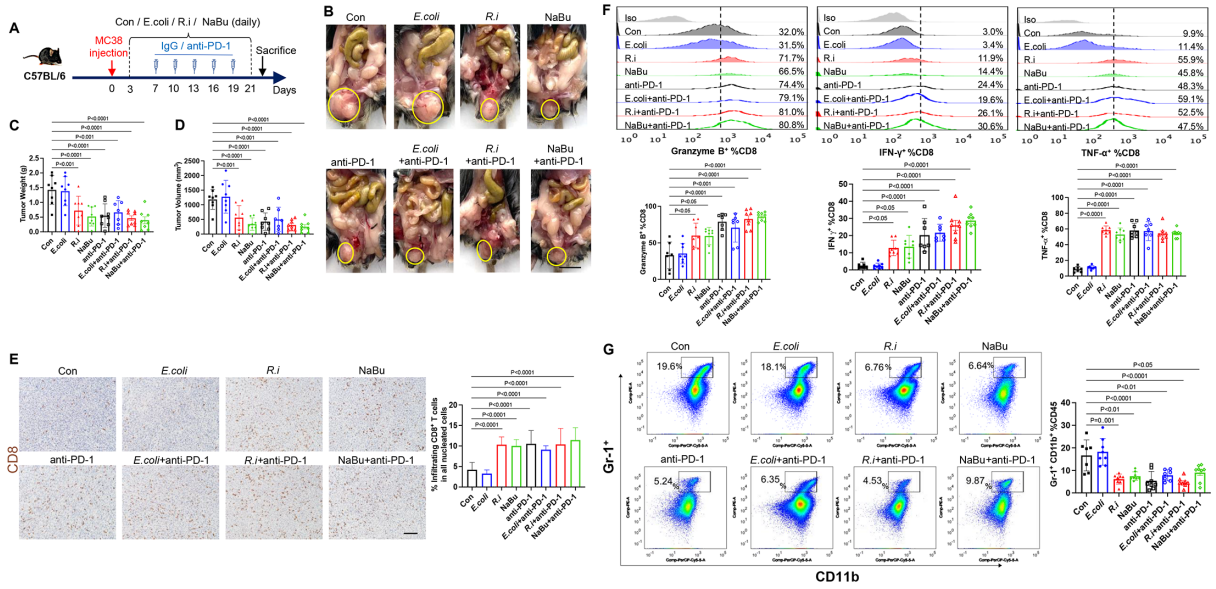

Figure 5 *Roseburia intestinalis (R.i)* and butyrate restrict MC38 orthotopic tumour growth by directly boosting CD8$^+$ T cells. (A) Schematic diagram showing the experimental design and timeline of MC38 orthotopic model. (B) Representative MC38 rectum orthotopic tumour morphologies. (C) Tumour volume (mm^3) and (D) tumour weight. (E) Proportion of tumour infiltrating CD8$^+$ T cells in all nucleated cells of MC-38 orthotopic tumour tissues determined by immunohistochemistry. (F) Frequencies of granzyme B, interferon (IFN)-γ, tumour necrosis factor (TNF)-α within CD8$^+$ populations of tumours from control, *Escherichia coli*-treated and *R.i*-treated C57BL/6J mice. (G) Frequencies of MDSC from tumour tissues in control, *E. coli*-treated and *R.i*-treated C57BL/6J mice measured by flow cytometry. Con, control; PD-1, programmed cell death protein 1.

table 1. Gating strategy is illustrated in online supplemental figure 1.

Surface plasmon resonance binding assay

To investigate the binding affinity between TLR5 and butyric acid, the Biacore T200 biosensor (GE Healthcare) was used to perform surface plasmon resonance. TLR5 human recombinant protein (TP315293, OriGene, Maryland, USA) was immobilised on a sensor chip CM5 (10328391, GE Healthcare) using an amine coupling kit (BR-1000-50, GE Healthcare) for 7 min, with a flow rate of 10 μL/min, resulting in a final ligand coupling of approximately 8500 response units (RU). Different concentrations of butyric acid (15.635, 31.25, 62.5, 125, 250, 500, 1000 μM) in pH 7.4 PBS were introduced using a microflow system. Association was allowed for 120 s at 30 μL/min, followed by dissociation for 200 s at 30 μL/min using a buffer solution wash, and regeneration for 30 s at 30 μL/min using glycine-HCl (10 mM). All binding experiments were conducted at 25°C, and the Biacore T200 evaluation software V.3.1 was used to determine the binding affinity.

Receptor-ligand interaction analysis

To analyse the TLR5 receptor-butyrate interactions, a molecular docking analysis was conducted. The three-dimensional structure of butyrate was obtained from the PubChem database (Compound CID: 104775) in SDF format. The structure was minimised and constructed in ChemDraw Ultra V.12.0[13] and converted into PDB format using PyMOL visualisation software. The crystal structure of TLR5 (PDB code: 3J0A) was downloaded from the Protein Data Bank. MGLTools 1.5.6 from AutoDock Vina 1.1.2 programme was used for processing TLR5,[14] while AutoDock was used for docking analysis. The docking runs were performed at a radius of 15 Å with specific coordinates x-axis: 52.981, y-axis: 63.073 and z-axis: 65.640. The top five results with the highest binding energy values were selected. Additionally, two-dimensional ligand-protein interaction diagrams were used to analyse hydrophobic interactions with LigPlus software,[15] calculating the number of van der Waals contacts of non-polar atoms.

Pull-down assay

Jurkat E6.1 cell was lysed with the pull-down buffer (50 mM Tris-HCl pH 7.4, 200 mM NaCl and 0.05% Tween-20) containing protease inhibitors. The lysate was then incubated with either the anti-TLR5 antibody (ab13876, abcam) or mouse IgG (sc-2027, Santa Cruz, California, USA) with or without 10 mM sodium butyrate at 4°C overnight while gently rotating in the pull-down buffer. The mixture was then incubated with Dynabeads Protein G beads (Invitrogen) for 2 hours at room temperature. Following this, samples were thoroughly washed with pull-down buffer 5 times and pull-down buffer without Tween-20 4 times before being eluted with 50 mM glycine (pH 2.8). A small portion of the eluate was used for western blot analysis to confirm successful pull-down of TLR5 while the remainder was used for liquid chromatography-mass spectrometry analysis to detect the level of butyrate binding to TLR5.

Statistical analyses

All measurements are shown as mean±SD. Independent Student's t-test was used to compare the difference between two groups, and multiple t-tests were used to compare the difference at different timepoints or stages between two groups. Two-way analysis of variance (ANOVA) was used to compare the difference among three groups, and one-way ANOVA with Turkey's multiple comparison was used to compare the difference among three or more groups. The χ^2 test was used to evaluate the proportion of tumour incidence between groups. Two-tailed p value <0.05 was considered statistically significant. Additional methods are provided in online supplemental file 1.

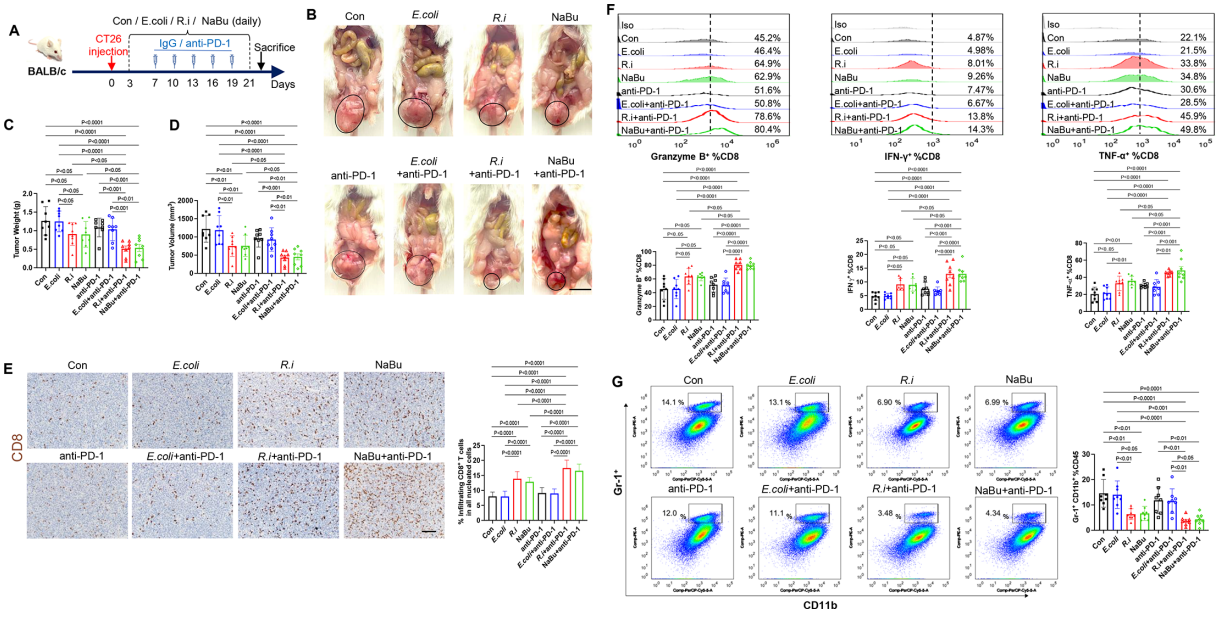

Figure 6 *Roseburia intestinalis (R.i)* and butyrate treatments are effective in CT26 orthotopic tumour via CD8$^+$ T cells independently from antiprogrammed cell death protein 1 (anti-PD-1) therapy. (A) Schematic diagram showing the experimental design and timeline of CT26 orthotopic model. (B) Representative CT26 rectum orthotopic tumour morphologies. (C) Tumour volume (mm^3) and (D) tumour weight. (E) Proportion of tumour infiltrating CD8$^+$ T cells of CT-26 orthotopic tumour in all nucleated cells determined by immunohistochemistry. (F) Frequencies of granzyme B, interferon (IFN)-γ, tumour necrosis factor (TNF)-α within CD8$^+$ populations of tumours from control, *Escherichia coli*-treated and *R.i*-treated BALB/c mice. (G) Frequencies of MDSC from tumour tissues in control, *E. coli*-treated and *R.i*-treated BALB/c mice measured by flow cytometry. Con, control.

RESULTS

R. intestinalis is depleted in stools of patients with CRC

We first evaluated the abundance of *R. intestinalis* in our in-house cohort of 110 patients with CRC and 112 healthy controls (online supplemental table 2). *R. intestinalis* was significantly depleted in faecal samples of patients with CRC compared with healthy controls (online supplemental figure 2A). For verification, we retrieved four published metagenomic datasets of 334 patients with CRC and 463 healthy controls.[16–19] The abundance of *R. intestinalis* was consistently decreased in all cohorts of patients with CRC (online supplemental figure 2B), thus confirming the depletion of *R. intestinalis* in CRC.

R. intestinalis inhibits CRC tumourigenesis in two different mouse models

The role of *R. intestinalis* in CRC tumourigenesis was first evaluated in *Apc*$^{Min/+}$ mice, receiving orally gavage with *R. intestinalis*, *E. coli* strain MG1655 or PBS for 6 weeks (figure 1A). *R. intestinalis* significantly reduced colon tumour incidence (figure 1B,C), tumour number and load (figure 1D, online supplemental figure 3) compared with mice treated with *E. coli* or PBS, respectively. *R. intestinalis*-treated mice also had lower dysplasia score with significantly less Ki-67-positive cells in both tumour and non-tumour colon tissues (figure 1E). Meanwhile, mouse body weight (online supplemental figure 4A), liver function (serum alanine aminotransferase and aspartate aminotransferase) and renal function (serum blood urea nitrogen and creatinine) (online supplemental figure 4B) were not altered with *R. intestinalis* treatment.

For validation, another mouse model with carcinogen-induced CRC (AOM) was used with 30 weeks administration of *R. intestinalis* (figure 1F). Similar to the findings of *Apc*$^{Min/+}$ mice, *R. intestinalis* significantly suppressed colorectal tumourigenesis with decreased tumour incidence (figure 1G,H), tumour number and load (figure 1I) as compared with controls. Lower dysplasia score and less Ki-67-positive cells were also observed in *R. intestinalis*-treated AOM mice (figure 1J). Collectively, our consistent results from two CRC mouse models demonstrated the suppressive role of *R. intestinalis* against colorectal tumourigenesis.

R. intestinalis improves gut barrier function in mice

Gut barrier dysfunction is known to play a pivotal role in CRC. We therefore examined the gut barrier integrity in *Apc*$^{Min/+}$ mice treated with *R. intestinalis*. *R. intestinalis* significantly reduced intestinal permeability as evidenced by decreased serum FITC-dextran level (figure 2). The protein expression of tight junction proteins ZO-1 and claudin-3 was also significantly increased in the colon tissues of *R. intestinalis*-treated mice, compared with mice treated with *E. coli* or PBS control (figure 2B). The upregulation of these genes in colon tissues was confirmed by IHC staining (figure 2C). Taking together, *R. intestinalis* could improve gut barrier function in CRC mice.

R. intestinalis culture medium suppresses the growth of CRC cells and patient-derived organoids

To investigate the tumour-suppressive mechanism of *R. intestinalis*, we first cocultured human CRC cell lines HCT116, LoVo and SW480, as well as a normal colon epithelial cell line NCM460, with live or pasteurised *R. intestinalis*, *E. coli* or broth control. However, neither live (online supplemental figure 5A) nor pasteurised (online supplemental figure 5B) *R. intestinalis* showed any difference in cell viability, indicating that *R. intestinalis* itself has no effect on CRC cell growth. We speculated that the tumour-suppressive role of *R. intestinalis* is attributed to its derivatives, and therefore treated CRC cells with *R.i* CM. *R.i* CM (5% vol/vol) significantly inhibited the cell viability of HCT116, LoVo and SW480, but not the normal colon cell line NCM460 (figure 3A). Similarly, *R.i* CM treatment reduced

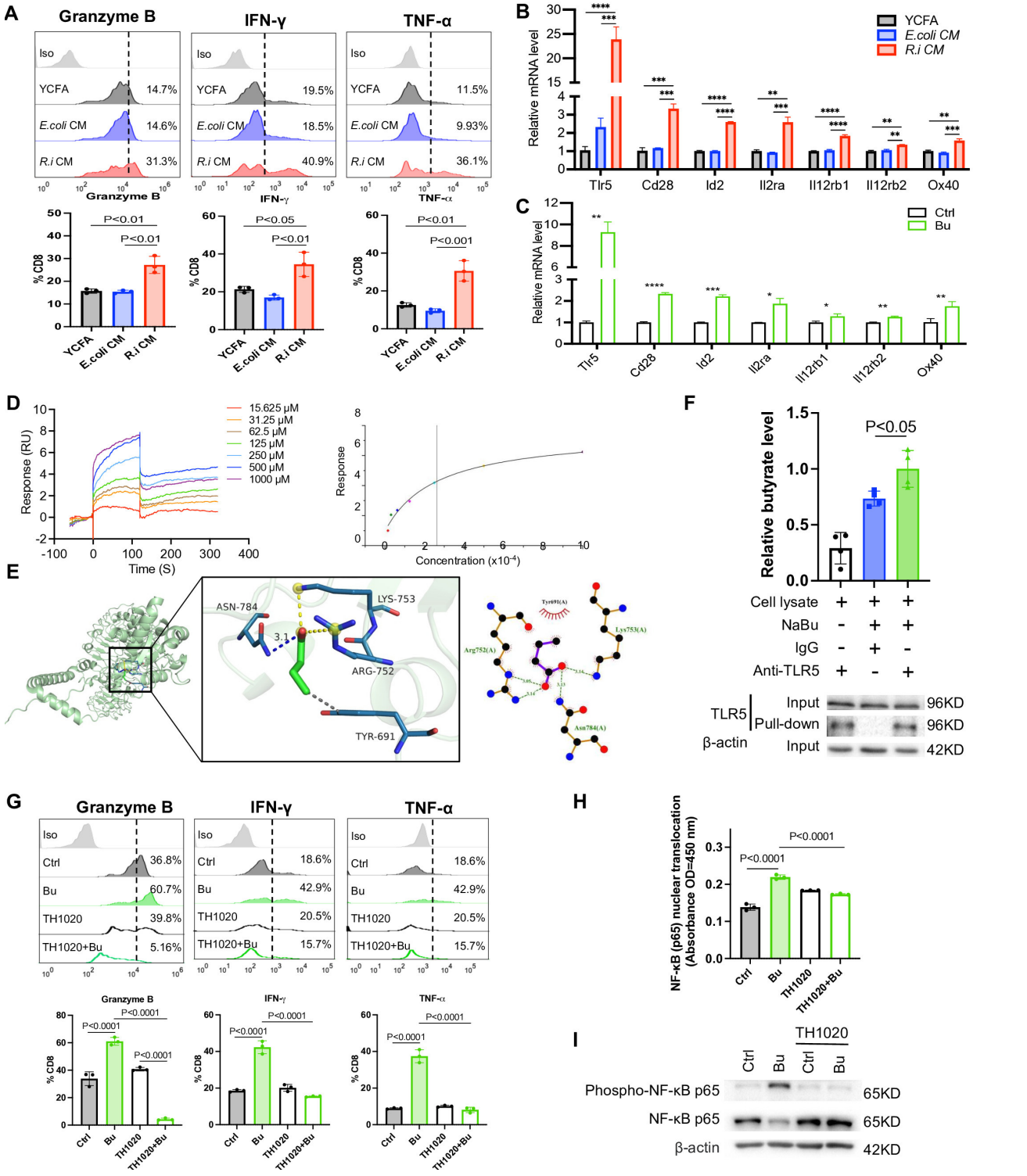

Figure 7 Comparable dosage of butyrate in *Roseburia intestinalis cultured medium* (*R.i* CM) suppresses colorectal cancer cells by direct CD8$^+$ T cell boosting in vitro. (A) *R.i* CM directly boosted granzyme B$^+$, interferon (IFN)-γ$^+$, tumour necrosis factor (TNF)-α$^+$ CD8$^+$ T cells isolated from human peripheral blood mononuclear cells (PBMC). (B) The messenger RNA (mRNA) expression level of significant changed receptors on CD8$^+$ T cells after treatment with *R.i* CM or (C) butyrate. (D) Binding affinity between toll-like receptor 5 (TLR5) and butyric acid was measured by surface plasmon resonance (left), affinity of TLR5 to butyric acid was 264 μM (right). (E) Representative structure of butyrate and TLR5 after molecular docking. The structure of TLR5 is represented in green and the butyrate is shown as stick in the centre (left). Relative interactions between butyrate and four amino acids of TLR5 generated by LigPlot (right). (F) Jurkat E6.1 T cell lysate incubation with anti-TLR5 or mouse IgG, together with or without 10 mM NaBu in pull-down buffer. Elute was evaluated by liquid chromatography-mass spectrometry (upper) and western blot analysis (down). (G) granzyme B$^+$, IFN-γ$^+$, TNF-α$^+$ CD8$^+$ T cells isolated from human PBMC were directly boosted by comparable dosage of butyrate and abolished by TLR5 antagonist TH1020. (H) Nuclear factor kappa B (NF-κB) (p65) nuclear translocation determined by NF-κB (p65) transcription factor assay. (I) Phospho-NF-κB p65 protein expression level of CD8$^+$ T cells isolated from human PBMC after butyrate treatment with or without TH1020 inhibition. *E. coli, Escherichia coli;* YCFA, yeast casitone fatty acids broth. *, P<0.05; **, P<0.01; ***, P<0.001; ****, P<0.0001.

colony formation (figure 3B) and proliferation (figure 3C), but increased both early and late apoptosis in CRC cells (figure 3D), as well as the protein expression of apoptosis markers cleaved caspase-7 and cleaved poly (ADP-ribose) polymerase (figure 3E). *R.i* CM also inhibited cell cycle G1-S phase transition with an increased proportion at G0/G1 phase and decreased in S phase in CRC cells (figure 3F). In keeping with this, the protein expression of cell cycle markers CDK6 was decreased and p27 Kip1 was increased by *R.i* CM (figure 3G). Moreover, *R.i* CM significantly suppressed the growth of organoids derived from patients with CRC (figure 3H). Altogether, these results suggested that molecules produced by *R. intestinalis* inhibit the growth of CRC cell lines and patient-derived organoids.

Butyrate is the functional tumour-suppressive metabolite produced by *R. intestinalis*

To determine the functional antitumour molecules generated by *R. intestinalis*, we separated *R.i* CM into two different fractions with molecular weight <3 kDa or >3 kDa. We found that only *R.i* CM with <3 kDa fraction exhibited suppressive effects on all three CRC cell lines HCT116, LoVo and SW480, but not in normal epithelial cell line NCM460 (figure 4A). This was not observed in *R.i* CM with >3 kDa fraction. *R.i* CM with <3 kDa fraction was therefore subjected to untargeted metabolomics profiling by LC-MS/MS, and butyric acid emerged as one of the most differentially enriched metabolites, compared with broth control (figure 4B). Subsequent targeted metabolomics analysis using GC-MS identified short-chain fatty acids (SCFAs) (online supplemental figure 6), confirming the substantial increase of butyric acid concentration to approximately 2000 µg/mL in the <3 kDa fraction of *R.i* CM (figure 4C). The elevation of butyric acid was further confirmed in stools of $Apc^{Min/+}$ and AOM-induced CRC mice receiving *R. intestinalis* supplementation (figure 4D).

The direct suppressive effect of butyrate was then assessed in vitro. The growth of CRC cells was significantly inhibited (figure 4E), together with increased apoptosis (figure 4F) and inhibited G1-S phase progression (figure 4G), by butyrate treatment with a comparable concentration (1 mM) in 5% *R.i* CM. Apart from butyric acid, inosine was also identified by untargeted metabolomics profiling as the top differentially enriched metabolites in *R.i* CM with <3 kDa fraction (online supplemental figure 7A). The concentration of inosine in *R.i* CM was around 8 µg/mL (online supplemental figure 7B). However, the comparable dosage of inosine in *R.i* CM had no significant suppressive effect on the growth of CRC cells (online supplemental figure 8A–C).

We further tested the association of *R. intestinalis* and butyric acid with colorectal tumourigenesis in human patients with CRC. Metabolomic profiling was performed on human faecal samples from our in-house cohort with 118 patients with CRC and 128 healthy controls,[20] which confirmed the significant depletion of butyric acid in patients with CRC (online supplemental figure 9A). *R. intestinalis* depletion was also observed in patients with CRC from this cohort (online supplemental figure 9B).[20] Collectively, these findings indicated that butyrate is the major metabolite responsible for the tumour-suppressive function of *R. intestinalis*.

R. intestinalis and butyrate improve anti-PD-1 efficacy in orthotopic CRC mouse models

From a published metagenomic dataset,[21] we found that *R. intestinalis* was significantly enriched in stool samples of 75 immune checkpoint blockade responders compared with 258 non-responders (online supplemental figure 10). We therefore tested whether *R. intestinalis* and butyrate could enhance immunotherapy efficacy against CRC. Oral gavage of *R. intestinalis*, sodium butyrate or *E. coli* was started 3 days after orthotopic injection of a mouse CRC cell line MC38 (MSI-high type), and anti-PD-1 therapy was initiated after the tumour was established (figure 5A). Both *R. intestinalis* and sodium butyrate significantly inhibited MC38 orthotopic tumour growth (figure 5B–D). Tumour growth was also suppressed in mice receiving anti-PD-1 monotherapy, while combining anti-PD-1 with *R. intestinalis* or sodium butyrate could not further enhance anti-PD-1 efficacy. *R. intestinalis* or sodium butyrate treatment of MC38 tumours increased infiltrating $CD8^+$ T cells (figure 5E) and granzyme B^+, IFN-γ^+ and TNF-α^+ $CD8^+$ T cells (figure 5F) while decreasing myeloid-derived suppressor cell (MDSCs) (figure 5G). MC38 syngeneic mice are known to be MSI-high with good immunotherapy response. Our findings suggested that *R. intestinalis* or butyrate has similar efficacy of tumour suppression as anti-PD-1 therapy in MSI-high type CRC allografts.

We then examined whether *R. intestinalis* or butyrate could also be effective in CT26 orthotropic mouse xenografts, which is a model with MSS and inherited immunotherapy resistance (figure 6A). As expected, CT26 orthotopic tumours were insensitive to anti-PD-1 therapy (figure 6B–D). Both tumour weight (figure 6C) and tumour size (figure 6D) were significantly reduced by the treatment of *R. intestinalis* or sodium butyrate compared with anti-PD-1 therapy and control groups. Moreover, the combination of *R. intestinalis* or sodium butyrate with anti-PD-1 further synergised the antitumour effects of *R. intestinalis* or sodium butyrate (figure 6B–D). Consistently, the proportion of infiltrating $CD8^+$ T cells (figure 6E) and granzyme B^+, IFN-γ and TNF-α^+ $CD8^+$ T cells was significantly increased in CT26 tumours with monotreatment of *R. intestinalis* or sodium butyrate (figure 6F), and their combination with anti-PD-1 showed additional effects on these immune cells (figure 6E–F). Treatment of *R. intestinalis* or sodium butyrate but not anti-PD-1 monotherapy also reduced the proportion of MDSCs in tumours (figure 6G). The increase of butyric acid was verified in the stools of both MC38 and CT26 orthotopic mice after administration of either *R. intestinalis* or sodium butyrate (online supplemental figure 11). These results collectively revealed that *R. intestinalis* and sodium butyrate are effective on facilizing anti-PD-1 therapeutic efficacy against CRC with MSS phenotype.

R. intestinalis-produced butyrate directly boosts cytotoxic $CD8^+$ T cell function

We examined the mechanism of how *R.i* CM and butyrate interact with $CD8^+$ T cells to modulate the antitumour immunity. T cells isolated from human PBMC or mouse spleen were treated with or without *R.i* CM or butyrate (1 mM). Both *R.i* CM and butyrate treatment promoted the production of granzyme B, IFN-γ and TNF-α by $CD8^+$ T cells (figure 7A, online supplemental figure 12). To understand their mechanistic association with $CD8^+$ T cells, the messenger RNA (mRNA) expression of receptors and transporters on $CD8^+$ T cells including *GPR43*, *SLCL6A1* and *TLR1–6* was examined after *R.i* CM treatment.[22–26] *R.i* CM did not change the expression of SCFAs receptors or transporters, but altered the expression of genes associated with effector T cells like *ID2*, *IL2RA* and *CD28* (figure 7B, online supplemental figure 13A). Particularly, the mRNA expression of pattern recognition receptor *TLR5* was over 10 times higher in *R.i* CM-treated $CD8^+$ T cells compared with

those treated with *E. coli* CM or YCFA control. Consistently, the mRNA expression of *TLR5* was significantly higher in butyrate-treated $CD8^+$ T cells compared with controls (figure 7C, online supplemental figure 13B). We confirmed that butyrate could bind to TLR5 receptor on $CD8^+$ T cells with an affinity of 264 μM by surface plasmon resonance (figure 7D). Butyrate was able to dock into the TLR5 catalytic site and the best docking conformation of complex had a binding energy of −3.5 kcal/mol (figure 7E), indicating that butyrate could spontaneously bind to the active pocket of TLR5. The butyrate-TLR5 physical interaction was confirmed by pull-down assay (figure 7F). To validate our findings, a selective TLR5 antagonist TH1020 was used to inhibit TLR5 signalling in $CD8^+$ T cells. TH1020 abolished the enhanced T cell response induced by butyrate, as evidenced by decreased production of granzyme B, IFN-γ and TNF-α in $CD8^+$ T cells (figure 7G). These results collectively suggested that *R. intestinalis*-produced butyrate promotes $CD8^+$ T cell activation through direct binding to TLR5 receptor on $CD8^+$ T cells.

NF-κB signalling is well-established as the downstream pathway of TLR5. Butyrate promoted nuclear translocation of NF-κB (p65) and its transcription factor DNA binding ability, as shown in $CD8^+$ T cell nuclear extracts (figure 7H). Butyrate also enhanced the expression of phospho-NF-κB (p65) in $CD8^+$ T cells, whereas such increase was reversed by TH1020 (figure 7H,I). Altogether, *R. intestinalis* produced butyrate to boost cytotoxic $CD8^+$ T cell function through activating the TLR5-NF-κB pathway.

DISCUSSION

In this study, we elucidated the protective role of *R. intestinalis* against colorectal tumourigenesis. The abundance of *R. intestinalis* in the gut microbiota of patients with CRC was found to be depleted in previous studies.[16–19] We also confirmed the depletion of *R. intestinalis* in our in-house CRC cohort. Of note, although its depletion has been frequently reported, the mechanism of how *R. intestinalis* protects against colorectal tumourigenesis remains completely unknown. Here, using two different mouse models (transgenic $Apc^{Min/+}$ and carcinogen AOM-induced CRC), for the first time we illustrated the tumour-suppressive function of *R. intestinalis* in vivo (figure 1). Moreover, gut barrier dysfunction plays a crucial role in CRC, of which increased intestinal permeability allows more pathogenic microbes and their derivatives to have easier access to the bloodstream, thereby contributing to microbial dissemination and metastasis.[27] Consistently, our results revealed the impairment of gut barrier in CRC mice, whereas *R. intestinalis* supplementation could significantly improve gut barrier integrity (figure 2).

We identified that the tumour-suppressive function of *R. intestinalis* is attributed to its derived metabolites (figure 3). To date, various antitumour mechanisms of probiotics have been discovered. Some of them exhibit anti-CRC effects by secreting protein derivatives,[28] while the others including *R. intestinalis*, produce metabolites to abolish colorectal tumourigenesis.[29] Through metabolomic profiling, we found that butyrate is the major antitumour metabolite produced by *R. intestinalis* (figure 4). Butyrate is an SCFA known to be negatively correlated with CRC incidence,[20] and accumulated evidence has demonstrated its diverse protective mechanisms against colorectal tumourigenesis. For instance, butyrate could epigenetically act as a histone deacetylase inhibitor to inhibit tumour cell proliferation,[30] while *Clostridium butyrium*, the major butyrate producer in the human gut, dampens CRC development by downregulating the oncogenic WNT signalling pathway.[31] In this study, our results clearly revealed that *R. intestinalis* is a butyrate-producing bacteria, and its derived butyrate could facilitate the direct killing of tumour cells with minimal effects on normal colon epithelial cells.

Apart from tumour cells, we illustrated a link between *R. intestinalis* and antitumour immunity. The gut microbiota is well-recognised for its influence on immunotherapy efficacy. Indeed, we confirmed the enrichment of *R. intestinalis* in immune checkpoint blockade responders from a published metagenomic dataset,[21] while faecal butyrate concentration was reported to be associated with anti-PD-1 efficacy in solid cancer.[32] We therefore tested the correlation between *R. intestinalis* or butyrate and anti-PD-1 therapy in two orthotopic mouse models bearing tumours with different CRC subtypes (MSI-high or MSS). Clinically, anti-PD-1 therapy is approved for patients with CRC with MSI-high subtype with a response rate of 40%.[33] For patients with MSS subtype, although they account for the majority of CRC cases (~85%), the immunological 'cold' tumour microenvironment in these patients has restricted the application of immunotherapy and how to improve their responsiveness to immune checkpoint blockade remains elusive.[34] Here, as expected, only mice bearing MSI-high but not MSS tumours responded to anti-PD-1 therapy (figures 5,6). Meanwhile, the combination of anti-PD-1 therapy with *R. intestinalis* or butyrate was effective to suppress the growth of MSS tumours with increased cytotoxic function of $CD8^+$ T cells. These results collectively indicated that *R. intestinalis* and its derived butyrate may be a promising adjuvant to patients with CRC who are resistant to anti-PD-1 therapy. Moreover, we observed that *R. intestinalis* or butyrate alone is sufficient to induce shrinkage of MSI-high and MSS tumours, thus suggesting the feasibility to leverage probiotics as a direct treatment of CRC.

We examined the mechanism of how *R. intestinalis*-derived butyrate interacts with antitumour $CD8^+$ T cells. G protein-coupled receptors (GPR)41, GPR43 and GPR109A are the major receptors on colon epithelial cells responsible for sensing butyrate and other SCFAs.[35] However, we observed that their expressions on $CD8^+$ T cells are not altered by butyrate. Similarly, a previous study reported that GPR blockade does not impair the effects of butyrate on functional $CD8^+$ T cells.[26] These findings therefore indicated that GPRs are dispensable for butyrate-mediated effects on $CD8^+$ T cells. Instead, we identified the significant upregulation of TLR5 on $CD8^+$ T cells and confirmed that TLR5 is a butyrate receptor by surface plasmon resonance and pull-down assay (figure 7). TLR5 is a receptor expressed on epithelial and immune cells specifically recognising flagellin on bacteria,[36] whereas currently there is a lack of studies reporting its interaction with microbial metabolites. Shen *et al* discovered that *R. intestinalis* stimulates TLR5 on intestinal epithelial cells to inhibit chronic inflammation.[37] In comparison, for the first time we revealed that *R. intestinalis*-derived butyrate but not *R. intestinalis* itself could directly bind to TLR5 on $CD8^+$ T cells to enhance their cytotoxic functions. Altogether, our results suggested a novel link between butyrate and a well-studied innate immune receptor, which may provide the basis for new therapeutic strategies to boost the antitumour immunity.

In summary, we observed significant depletion of gut *R. intestinalis* and butyrate in patients with CRC. By using multiple mouse models, we demonstrated the tumour-suppressive roles of *R. intestinalis* against two different subtypes of CRC including MSI-high and MSS tumours. *R. intestinalis* exhibits its antitumour function by producing butyrate. Both *R. intestinalis* and butyrate enhance the efficacy of anti-PD-1 therapy in CRC. Mechanistically, we revealed the direct binding of *R. intestinalis*-derived butyrate to TLR5 on $CD8^+$ T cells, thereby boosting

the antitumour immunity. Thus, *R. intestinalis* is a promising probiotic supplement, which potentially open a new avenue to improve treatment efficacy in patients with CRC, particularly for those with anti-PD-1 therapy resistance.

Twitter Sunny H Wong @sunnyheiwong

Contributors XK was involved in the study design, conducted experiments and drafted the manuscript; CL and YD performed bioinformatics analysis; YN performed histological analysis; FJ operated LC-MS/MS; HCHL and LJ performed animal experiments; JJYS commented on the study; SW and JY conceived, supervised the study and revised the manuscript. JY acts as the guarantor of the study.

Funding This project was supported by Research Talent Hub-Innovation and Technology Fund Hong Kong (ITS/177/21FP); RGC Research Impact Fund Hong Kong (R4032-21F); Shenzhen-Hong Kong-Macao Science and Technology Programme (Category C) Shenzhen (SGDX20210823103535016); Vice-Chancellor's Discretionary Fund Chinese University of Hong Kong (4930775); Singapore Ministry of Health's National Medical Research Council under its Clinician Scientist Individual Research Grant (CS-IRG) (MOH-CIRG23jan-0001), NTU Start Up Grant (021337-00001, 021281-00001), Centre for Microbiome Medicine, and Wang Lee Wah Memorial Fund.

Competing interests None declared.

Patient and public involvement Patients and/or the public were not involved in the design, or conduct, or reporting, or dissemination plans of this research.

Patient consent for publication Not applicable.

Ethics approval All experimental procedures were approved by the Chinese University of Hong Kong Animal Ethics Committee.

Provenance and peer review Not commissioned; externally peer reviewed.

Data availability statement Data are available in a public, open access repository. Not applicable.

ORCID iDs
Harry Cheuk Hay Lau http://orcid.org/0000-0003-3581-2909
Joseph JY Sung http://orcid.org/0000-0003-3125-5199
Sunny H Wong http://orcid.org/0000-0002-3354-9310
Jun Yu http://orcid.org/0000-0001-5008-2153

REFERENCES

1 Siegel RL, Miller KD, Fuchs HE, *et al*. Cancer statistics, 2022. *CA Cancer J Clin* 2022;72:7–33.
2 Brahmer JR, Tykodi SS, Chow LQM, *et al*. Safety and activity of anti-PD-L1 antibody in patients with advanced cancer. *N Engl J Med* 2012;366:2455–65.
3 Dudley JC, Lin MT, Le DT, *et al*. Microsatellite instability as a biomarker for PD-1 blockade. *Clin Cancer Res* 2016;22:813–20.
4 Boland CR, Goel A. Microsatellite instability in colorectal cancer. *Gastroenterology* 2010;138:2073–87.
5 Iida N, Dzutsev A, Stewart CA, *et al*. Commensal bacteria control cancer response to therapy by Modulating the tumor Microenvironment. *Science* 2013;342:967–70.
6 Routy B, Le Chatelier E, Derosa L, *et al*. Gut Microbiome influences efficacy of PD-1-based Immunotherapy against epithelial tumors. *Science* 2018;359:91–7.
7 Vétizou M, Pitt JM, Daillère R, *et al*. Anticancer Immunotherapy by CTLA-4 blockade relies on the gut Microbiota. *Science* 2015;350:1079–84.
8 Zitvogel L, Daillère R, Roberti MP, *et al*. Anticancer effects of the Microbiome and its products. *Nat Rev Microbiol* 2017;15:465–78.
9 Koh A, De Vadder F, Kovatcheva-Datchary P, *et al*. From dietary fiber to host physiology: short-chain fatty acids as key bacterial metabolites. *Cell* 2016;165:1332–45.
10 Wang T, Cai G, Qiu Y, *et al*. Structural segregation of gut Microbiota between colorectal cancer patients and healthy volunteers. *ISME J* 2012;6:320–9.
11 Duncan SH, Hold GL, Barcenilla A, *et al*. Roseburia Intestinalis SP. Nov., a novel Saccharolytic, butyrate-producing bacterium from human Faeces. *Int J Syst Evol Microbiol* 2002;52(Pt 5):1615–20.
12 Nie K, Ma K, Luo W, *et al*. Roseburia Intestinalis: A beneficial gut organism from the discoveries in genus and species. *Front Cell Infect Microbiol* 2021;11:757718.
13 Cousins KR. Computer review of Chemdraw ultra 12.0. *J Am Chem Soc* 2011;133:8388.
14 Trott O, Olson AJ. Autodock vina: improving the speed and accuracy of docking with a new scoring function, efficient optimization, and Multithreading. *J Comput Chem* 2010;31:455–61.
15 Laskowski RA, Swindells MB. Ligplot+: multiple ligand-protein interaction diagrams for drug discovery. *J Chem Inf Model* 2011;51:2778–86.
16 Yu J, Feng Q, Wong SH, *et al*. Metagenomic analysis of Faecal Microbiome as a tool towards targeted non-invasive biomarkers for colorectal cancer. *Gut* 2017;66:70–8.
17 Wirbel J, Pyl PT, Kartal E, *et al*. Meta-analysis of fecal Metagenomes reveals global microbial signatures that are specific for colorectal cancer. *Nat Med* 2019;25:679–89.
18 Zeller G, Tap J, Voigt AY, *et al*. Potential of fecal Microbiota for early-stage detection of colorectal cancer. *Molecular Systems Biology* 2014;10:766.
19 Yachida S, Mizutani S, Shiroma H, *et al*. Metagenomic and Metabolomic analyses reveal distinct stage-specific phenotypes of the gut Microbiota in colorectal cancer. *Nat Med* 2019;25:968–76.
20 Coker OO, Liu C, Wu WKK, *et al*. Altered gut metabolites and Microbiota interactions are implicated in colorectal carcinogenesis and can be non-invasive diagnostic biomarkers. *Microbiome* 2022;10:35.
21 Derosa L, Routy B, Thomas AM, *et al*. Intestinal Akkermansia Muciniphila predicts clinical response to PD-1 blockade in patients with advanced non-small-cell lung cancer. *Nat Med* 2022;28:315–24.
22 Rangan P, Mondino A. Microbial short-chain fatty acids: a strategy to tune adoptive T cell therapy. *J Immunother Cancer* 2022;10:e004147.
23 Arens R, Schoenberger SP. Plasticity in programming of Effector and memory Cd8 T-cell formation. *Immunol Rev* 2010;235:190–205.
24 Salerno F, Turner M, Wolkers MC. Dynamic post-transcriptional events governing $Cd8^+$ T cell homeostasis and Effector function. *Trends Immunol* 2020;41:240–54.
25 Shyer JA, Flavell RA, Bailis W. Metabolic signaling in T cells. *Cell Res* 2020;30:649–59.
26 He Y, Fu L, Li Y, *et al*. Gut microbial metabolites facilitate anticancer therapy efficacy by Modulating cytotoxic $Cd8^+$ T cell immunity. *Cell Metab* 2021;33:988–1000.
27 Bertocchi A, Carloni S, Ravenda PS, *et al*. Gut vascular barrier impairment leads to intestinal bacteria dissemination and colorectal cancer metastasis to liver. *Cancer Cell* 2021;39:708–24.
28 Li Q, Hu W, Liu W-X, *et al*. Streptococcus Thermophilus inhibits colorectal tumorigenesis through Secreting β-Galactosidase. *Gastroenterology* 2021;160:1179–93.
29 Sugimura N, Li Q, Chu ESH, *et al*. *Lactobacillus Gallinarum* modulates the gut Microbiota and produces anti-cancer metabolites to protect against colorectal Tumourigenesis. *Gut* 2021;71:2011–21.
30 Donohoe DR, Collins LB, Wali A, *et al*. The Warburg effect dictates the mechanism of butyrate-mediated Histone Acetylation and cell proliferation. *Mol Cell* 2012;48:612–26.
31 Chen D, Jin D, Huang S, *et al*. Clostridium Butyricum, a butyrate-producing Probiotic, inhibits intestinal tumor development through Modulating WNT signaling and gut Microbiota. *Cancer Lett* 2020;469:456–67.
32 Nomura M, Nagatomo R, Doi K, *et al*. Association of short-chain fatty acids in the gut Microbiome with clinical response to treatment with Nivolumab or Pembrolizumab in patients with solid cancer tumors. *JAMA Netw Open* 2020;3:e202895.
33 Le DT, Durham JN, Smith KN, *et al*. Mismatch repair deficiency predicts response of solid tumors to PD-1 blockade. *Science* 2017;357:409–13.
34 Lizardo DY, Kuang C, Hao S, *et al*. Immunotherapy efficacy on mismatch repair-deficient colorectal cancer: from bench to bedside. *Biochim Biophys Acta Rev Cancer* 2020;1874:188447.
35 Sivaprakasam S, Prasad PD, Singh N. Benefits of short-chain fatty acids and their receptors in inflammation and carcinogenesis. *Pharmacol Ther* 2016;164:144–51.
36 Hayashi F, Smith KD, Ozinsky A, *et al*. The innate immune response to bacterial Flagellin is mediated by toll-like receptor 5. *Nature* 2001;410:1099–103.
37 Shen Z, Luo W, Tan B, *et al*. Roseburia Intestinalis stimulates Tlr5-dependent intestinal immunity against Crohn's disease. *EBioMedicine* 2022;85:104285.